International Journal of Electrical, Electronic and Communication Sciences
ISSN: 2517-9438
Vol:8, No:8, 2014

Diagnosis of Induction Machine Faults by DWT

Hamidreza Akbari

***Abstract*—**In this paper, for detection of inclined eccentricity in an induction motor, time–frequency analysis of the stator startup current is carried out. For this purpose, the discrete wavelet transform is used. Data are obtained from simulations, using winding function approach. The results show the validity of the approach for detecting the fault and discriminating with respect to other faults.

***Keywords*—**Induction machine, Fault, DWT.

I. Introduction

MECHANICAL faults occur because of damage to the mechanical elements of electrical machine such as bearings and gear-box. The mechanical faults are responsible for more than 50% of all failures in induction machines [1], [2].

The most important mechanical fault is eccentricity [3]. There are different methods for the detection of mechanical faults, such as monitoring the vibration, acoustic noise analysis, temperature measurement, radio frequency emission monitoring and motor current signature analysis (MCSA) [4]. Among all these methods, MCSA is one of the most popular methods [4]. Some researchers have applied the discrete wavelet transform (DWT) to the stator startup current in order to detect the presence of broken rotor bars in induction machines [5], [6]. Few works have been done regarding the application of wavelet theory for the detection of eccentricities and they are mainly focused in the variations that the fault causes on particular parameters of the wavelet transform, such as the wavelet packet coefficients [7], [8]. In [9] DWT analysis of the stator startup current is proposed as a way to detect the presence of dynamic eccentricity in induction machines.

This paper proposes a method allows the detection of the presence of the inclined eccentricity fault in two different ways; a qualitative one, based on the identification of the characteristic pattern that arises in the wavelet signals and a quantitative approach, focused on the analysis of the energy of the signals.

To confirm the proposed method, a three phase induction motor has been simulated under healthy, broken bar and inclined eccentricity conditions using winding function approach.

II. Inclined Eccentricity in Induction Machines

There are three types of air-gap eccentricity; Static, dynamic and mixed eccentricity [10], [11]. Static eccentricity (SE) occurs when the rotor rotates about its own centerline, but this centerline does not coincide with that of the stator bore. Dynamic eccentricity (DE) occurs when the rotor geometric center is not at the center of rotation, producing consequently an air-gap periodic variation as a rotor position function. In mixed eccentricity (ME) both rotor symmetrical and mechanical rotation centerlines are displaced individually in respect to the stator symmetrical centerline.

As shown in Fig. 1, inclined eccentricity is caused by improper alignment of right and left bearing centers so that the rotor's geometric axis is not parallel to that of the stator. Therefore, along the axial direction, the degree of eccentricity is not constant.

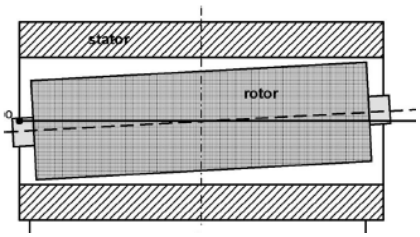

Fig. 1 Inclined eccentricity in an induction machine [12]

Fig. 2 shows the variation of air gap eccentricity coefficients in different positions. δ_i is the static eccentricity coefficient in the back side or front side of the rotor.

The air gap function is as follows:

$$g_{mis}(\phi, z, \theta_r) = g_h(\phi, z, \theta_r)(1-\delta_s(z)\cos(\phi-\phi_0)) \quad (1)$$

where

$$\delta_s(z) = \frac{-2\delta_i}{l}(z-\frac{l}{2}) \quad (2)$$

$g_h(\phi, z, \theta_r)$ is the air gap function in healthy machine. Mean radius is as follows:

$$r_{av}(\phi, z, \theta_r) = r_{sta}(\phi) - \frac{g_{mis}(\phi, z, \theta_r)}{2} \quad (3)$$

Hamidreza Akbari is with the Department of Electrical Engineering, Yazd Branch, Islamic Azad University, Yazd, Iran. (Tel: +98(351)8117548, Fax: +98(351) 8117548; e-mail: h.akbari@iauyazd.ac.ir).

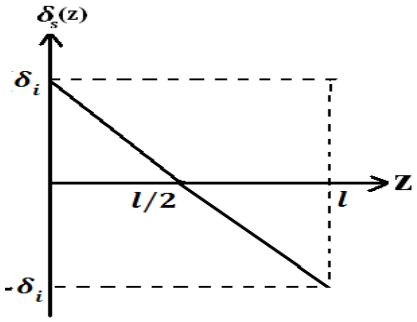

Fig. 2 Variation of eccentricity coefficients in different positions

Fig. 3 shows an elementary machine with asymmetrical inclined rotor. The occurrence of this fault means the separation of the rotor axis from the symmetrical inclined rotor [13].

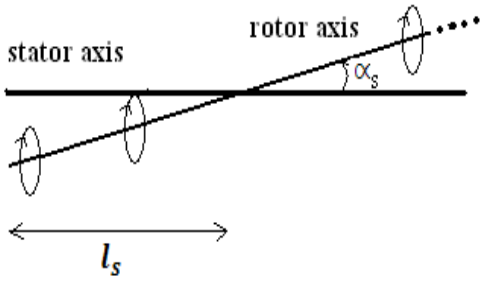

Fig. 3 Asymmetrical inclined rotor in machine [13]

The static eccentricity coefficient is the function of the position along the axial direction. Through geometric analysis on Fig. 3, it is easy to show that the static eccentricity level at any point along the axial direction as

$$\delta_s(z) = tan(\alpha_s)(z - l_s)/g_0 \tag{4}$$

α_s is the inclined angle of the rotor and l_s is the shaft misalignment level.

III. Calculation of Inductances under Axial Nonuniformity Conditions

In the induction machine, the 2-DMWF, $N(\phi, z, \theta_r)$, can be defined for each stator winding and each rotor loop composed by two bars [14].

$$N(\phi, z, \theta_r) = n(\phi, z, \theta_r) - \frac{1}{2\pi L(g^{-1}(\phi, z, \theta_r))} \times \int_{0_1}^{2\pi L} \int_{0}^{} n(\phi, z, \theta_r) g^{-1}(\phi, z, \theta_r) dz d\phi \tag{5}$$

where g^{-1}, r and n are inverse air gap, mean radius and turn functions respectively. L, θ_r, ϕ and z are rotor length, rotor angle, arbitrary angle in stator reference frame and position of inclined length respectively.

Magnetic motive force (MMF) distribution in the air gap, produced by a current i_A flowing in any coil A (stator windings or rotor loops) is as follows:

$$F_A(\phi, z, \theta_r) = N_A(\phi, z, \theta_r) i_A \tag{6}$$

So, a differential flux through a differential area in the air gap, $r(\phi, z, \theta_r) dz d\phi$, can be written as follows:

$$d\phi = \mu_0 F_A(\phi, z, \theta_r) g^{-1}(\phi, z, \theta_r) r(\phi, z, \theta_r) dz d\phi \tag{7}$$

Integrating the differential flux in the region covered by either a stator coil or a rotor loop, yields:

$$\phi_B = \mu_0 \int_{\Phi_1}^{\Phi_2} \int_{Z_1(\Phi)}^{Z_2(\Phi)} r(\phi, z, \theta_r) N_A(\phi, z, \theta_r) i_A g^{-1}(\phi, z, \theta_r) dz d\phi \tag{8}$$

$n_B(\phi, z, \theta_r)$ is equal to the coil turns in the region ($\phi_1 < \phi < \phi_2$, $z_1(\phi) < z < z_2(\phi)$) and zero otherwise. Therefore the total flux linking coil B, λ_B is obtained from multiplying (8) by $n_B(\phi, z, \theta_r)$ and integrating it over the whole surface:

$$\lambda_B = \mu_0 \int_{0_1}^{2\pi} \int_{0}^{L} r(\phi, z, \theta_r) n_B(\phi, z, \theta_r) N_A(\phi, z, \theta_r) \times i_A g^{-1}(\phi, z, \theta_r) dz d\Phi \tag{9}$$

Therefore, the mutual inductance of windings A and B, due to current i_a in the coil A ($L_{BA}(\theta_r)$), is

$$L_{BA}(\theta_r) = \frac{\lambda_B}{i_A} \tag{10}$$

$$L_{BA}(\theta_r) = \mu_0 \int_{0_1}^{2\pi L} \int_{0}^{} \frac{r(\phi, z, \theta_r) n_B(\phi, z, \theta_r) N_A(\phi, z, \theta_r)}{g(\phi, z, \theta_r)} dz d\phi \tag{11}$$

Inductances of induction machine can be calculated from (11) using geometrical characteristic of the machine.

A salient feature of modified winding function approach is its capability to simulate the mechanical asymmetry and fault of stator and rotor which has no restrictions about nonuniformities. Therefore, nonuniformity in all directions can be modeled by this approach. Also space harmonics of the windings MMF and slots harmonics are taken into account in the model. The winding function used in this paper takes into account the sinusoidal variation of MMF on the slots. Fig. 4 shows the turn function of the rotor loop1. All the inductances are computed at several rotor angular positions and stored within a computer file. The calculated inductances are used in a coupled electromagnetic model [15] for simulation and studying the frequency spectrum of the stator line current in the presence of inclined eccentricity. The electromagnetic coupling model of the machine circuits is solved using a 4th

and 5th order Runge-Kutta method. Specifications of the simulated motor have been summarized in Table I.

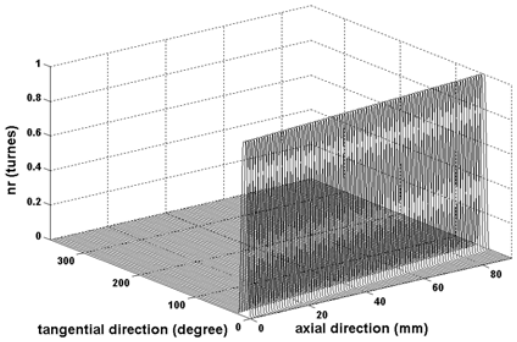

Fig. 4 Turn function of the rotor loop1, considering rotor skewing

TABLE I
SPECIFICATIONS OF SIMULATED MOTOR

Number of poles	4
Inner diameter of stator (mm)	90
Air gap length (mm)	0.3
Core length (mm)	90
Number of stator slots	36
Number of rotor slots	28
Rated voltage, V	380
Rated frequency, Hz	50
Rated power, hp	3

IV. DWT ANALYSIS

Applying the wavelet transform to the original signal divides the signal into two parts, the high-frequency part and the low frequency part. The low-frequency part is called an approximation of the original signal. A series of approximations can be obtained by reiterating such decompositions. The difference of the approximations between two successive decompositions is called the details. The approximation signal behaves as a low-pass filter whereas each wavelet signal behaves as a pass-band filter [16]. There is a certain overlap between bands due to the non-ideal characteristic of the wavelet filters, arising the problem of aliasing between bands. The use of a high-order wavelet reduces the problem of the overlap between frequency bands [16]-[18]. In this research, Daubechies 44 has been employed.

The components introduced in the current spectrum by the eccentricity can be detected using MCSA [4]. The equation describing the frequency components around the slot frequency are given by

$$f_h = f[(kR \pm n_d)(\frac{1-s}{p}) \pm v] \quad (12)$$

where n_d = 0 in the case of SE, and n_d = 1, 2, 3,… in the case of DE (n_d is known as the eccentricity order), f is the fundamental supply frequency, R is the number of rotor slots, s is the slip, p is the number of pole pairs, k is any integer, and v is the order of the stator time harmonics that are present in the power supply driving the motor (v = 1, 3, 5, etc.)

The frequency components around the supply frequency are given by,

$$f_h = f[1 \pm m(\frac{1-s}{p})] \quad (13)$$

A phase current during the startup transient was captured using a sampling frequency of 9 kHz for all the cases that were simulated. The DWT was computed for each case using MatLab Wavelet Toolbox. In order to get an approximation signal containing frequencies below the supply frequency, the number of decomposition levels that has to be considered is given by [5].

$$n_{dec} = \text{int}(\frac{\log(\frac{f_s}{f})}{\log(2)}) \quad (14)$$

The sampling frequency is 9 kHz, therefore the number of decomposition levels is obtained 7. Table II shows the frequency bands corresponding to the approximation and detail signals resulting from the 7-level DWT analysis.

TABLE II
FREQUENCY BANS FOR THE APPROXIMATION AND DETAIL SIGNALS RESULTING FROM THE 7-LEVEL DWT ANALYSIS

Frequency band	signal
0-35.15 Hz	a7
35.15-70.3 Hz	d7
70.3-140.6 Hz	d6
140.6-281.2 Hz	d5
281.2-562.4 Hz	d4
562.4-1124.8Hz	d3
1124.8-2249.6 Hz	d2
2249.6-4499.2Hz	d1

Fig. 5 shows the high-level signals resulting from the 7-level DWT analysis of the current for the cases of loaded machine under healthy, inclined eccentricity and broken rotor bar conditions, respectively. In the inclined eccentricity condition, one end is 0% SE and the other end is 50% SE.

Fig. 6 shows the high-level signals resulting from the 7-level DWT analysis of the current for the case of machine coupled to a load with a cyclically variable torque. The frequency of the torque oscillation is 25 Hz. It can be observed that the pattern created by the eccentricity is totally different from that appearing in other cases.

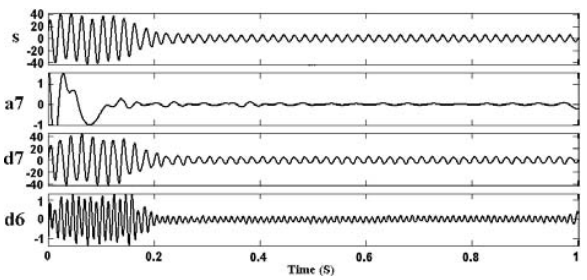

(a)

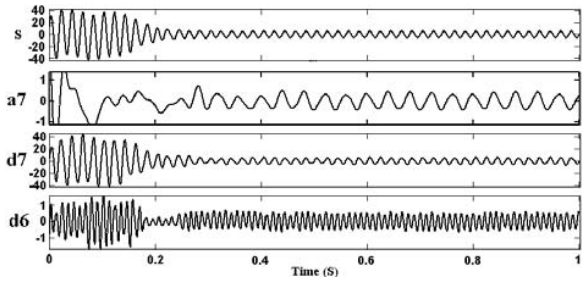

(b)

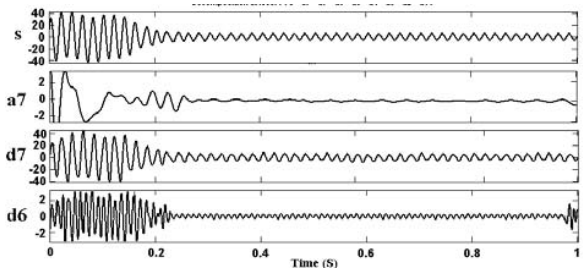

(c)

Fig. 5 DWT of the simulated startup current for the machine in fully loaded in (a) healthy (b) inclined eccentricity (c) two broken bar conditions

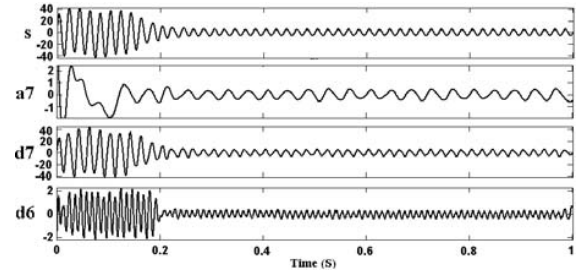

Fig. 6 DWT of the simulated startup current for the machine loaded with fluctuating torque

The frequencies given in (13) for m = 1 are function of the slip. As the slip changes during the startup transient from 1 to 0.03, the frequencies of those components will also change. Considering f=50 Hz, the component with negative sign will be

$$f_{h-} = 50(1 - \frac{1-s}{2}) = 25 + 25s \quad (15)$$

So the frequency of this component will decrease firstly from 50 Hz (S=1) to its steady-state value 25.75 Hz, for S=0.03. This means that, firstly, this component will be included within the wavelet signal d7, which contains frequencies between 35.15 and 70.3 Hz, and it will evolve later within signal a7 (0–35.15 Hz), reaching its steady-state value. The component with positive sign will be

$$f_{h+} = 50(1 + \frac{1-s}{2}) = 75 - 25s \quad (16)$$

This component evolutes during the startup transient from 50 Hz (S=1) to 74.25 Hz (S=0.03). Therefore, initially this component evolves within the signal d7. As its frequency gets nearer to the steady-state value, it comes into the signal d6, where it is reflected through the oscillations in that signal. Therefore a clear pattern created by these two components associated with the eccentricity fault arises. The pattern consists of the progressive increment in amplitude of the wavelet signals beside the one containing the fundamental component. The amplitudes of these signals increase during the transition between the startup transient and the steady-state, until reaching a constant value in stationary regime. The detection of this characteristic pattern constitutes a consistent evidence for the diagnosis of the fault from a qualitative point of view.

The analyses of the energies of the signals a7 and d6 can provide a tool for quantifying the degree of severity of the fault. We calculate energies of signals for four conditions and put results in the Table III. This energy is normalized by total signal energy like per unit systems.

TABLE III
ENERGIES OF A7 AND D6 IN DIFFERENT CONDITIONS

signal	healthy	10% ECC	25%ECC	50% ECC
A7	8.12×10^{-7}	$.95\times10^{-5}$	9.32×10^{-5}	9.22×10^{-3}
D6	1.02×10^{-5}	1.2×10^{-4}	2.1×10^{-3}	8.2×10^{-2}

Clear increments in the energy of these signals are observed as the severity of the fault increases. This fact allows the quantification of the degree of severity of the eccentricity fault.

V. CONCLUSIONS

In this paper, a method for the detection of inclined eccentricity in induction machines has been introduced. Winding function approach is used for providing the simulation data. The method is tested in different faulty and operating conditions. When inclined eccentricity is present in the machine, a characteristic pattern can be detected. This pattern is based on two components associated with the eccentricity within the wavelet signals adjacent to fundamental frequency. This pattern brings a qualitative way for detecting the presence of the fault, since it is completely different from that caused by other phenomena. In addition, the analysis of the energy of the wavelet signals can be used as a quantitative indicator of the degree of severity of the fault.

REFERENCES

[1] J. Faiz1, B. Ebrahimi, B. Akin, and H. Toliyat,"Finite-Element Transient Analysis of Induction Motors Under Mixed Eccentricity Fault," *IEEE Trans. Magnetics*, vol. 44, no. 1, January 2008.
[2] A. M. Trzynadlosky, "Diagnostic of mechanical abnormalities in induction motor using instantaneous electric power," in *Proc. 1997 Int. Electr. Machines Drives Conf.*, Milwaukee, WI, pp. 91–93.
[3] N. M. Elkasabgy, A. R. Eastman, and G. E. Dawson, "Detection of broken bar in the cage rotor on an induction machine," *IEEE Trans. Industry Application*, vol. 28, no. 1, pp. 165–171, Jan./Feb. 1992.

[4] S. Nandi,, H. Toliyat, and Xiaodong Li,*"* Condition Monitoring and Fault Diagnosis of Electrical Motors—A Review", *IEEE Trans. Energy Conversion*, vol. 20, no. 4, December 2005.
[5] J. Antonino-Daviu, M. Riera-Guasp, J. Roger-Folch, F. Martı´ nez-Gime´ and nez, A. Peris, "Application and optimization of the discrete wavelet transform for the detection of broken rotor bars in induction machines," *Applied and Computational Harmonic Analysi*s, vol. 21, no. 2, pp. 268–279, 2006.
[6] J.A. Antonino-Daviu, M. Riera-Guasp, J. Roger-Folch and M.P. Molina, "Validation of a new method for the diagnosis of rotor bar failures via wavelet transform in industrial induction machines," *IEEE Trans. Industry Applications*, vol. 42, no. 4, pp. 990–996, 2006.
[7] Z. Ye, A. Sadeghian and B. Wu, "Mechanical fault diagnostics for induction motor with variable speed drives using Adaptative Neurofuzzy Inference System," *Electric Power Systems Research*, vol. 76, no. 10, pp. 742–752, 2006.
[8] Z. Ye, B. Wu and A. Sadeghian, "Current signature analysis of induction motor mechanical faults by wavelet packet decomposition," *IEEE Transactions on Industrial Electronics*, vol. 50, no. 6, pp. 1217–1228,(2003.
[9] J. Antonino, P. Joverb, M. Rieraa, A. Arkkiob and J. Roger-Folch, "DWT analysis of numerical and experimental data for the diagnosis of dynamic eccentricities in induction motors", *Mechanical Systems and Signal Processing*, vol. 21, pp. 2575–2589, 2007.
[10] J. Faiz, I. T. Ardekani and H. A. Toliyat, "An evaluation of inductances of a squirrel-cage induction motor under mixed eccentric conditions," *IEEE Trans Energy Conversion*, vol. 18, no. 2, June 2003.
[11] M. Ojaghi and S. Nasiri, Modeling Eccentric Squirrel-Cage Induction Motors With Slotting Effect and Saturable Teeth Reluctances, IEEE Transactions on Energy Conversion, pp. 1-9, No. 99, DOI 10.1109/TEC.2014.2320823, 2014.
[12] Li ediadong and S. Nandi, "Performance analysis of a three phase induction machine with inclined static eccentricity ", *IEEE Trans. Industry Application*, vol. 43, no. 2, March 2007.
[13] Hamidreza Akbari," Modeling and Simulation of Induction Machines Under Misalignment Condition", *ICIEE,Dubai*, Oct. 2012.
[14] G. Bossio, C. D. Angelo, J. Solsona, G. Garcia and M. I. Valla, "A 2-D model of the induction machine: an extension of the modified winding function approach," *IEEE Trans. Energy Conversion*, vol. 19, no. 1, March 2004.
[15] Hamid A. Toliyat, T. A. Lipo, and J. C. White, "Analysis of a concentrated winding induction machine for adjustable speed drive applications, part-1(motor analysis)", *IEEE Trans. energy conversion*, vol. 6, pp. 679-692, Dec.1991.
[16] C.S. Burrus, R.A. Gopinath and H. Guo, *Introduction to Wavelets and Wavelet Transforms a Primer*, Prentice-Hall, Englewood Cliffs, NJ, 1998.
[17] R. Polikar, L. Udpa, S.S. Udpa and T. Taylor, "Frequency invariant classification of weld inspection signals," *IEEE Tranactions on Ultrasonics Ferroelectrics and Frequency Control* vol. 45, no. 3, pp. 614–625, 1998.
[18] T. Tarasiuk, "Hybrid wavelet-Fourier spectrum analysis," *IEEE Transactions on Power Delivery*, vol. 19, no. 3, pp. 957–964, 2004.